34th Annual International Conference of the IEEE EMBS
San Diego, California USA, 28 August - 1 September, 2012

Automatic Pterygium Detection on Cornea Images to Enhance Computer-aided Cortical Cataract Grading System

Xinting Gao[1], Wing Kee Damon Wong[1], Aloysius Wishnu Aryaputera[2], Ying Sun[2]
Ching-Yu Cheng[3], Carol Cheung[3] and Tien Yin Wong[3]

***Abstract*— In this paper, we present a new method to detect pterygiums using cornea images. Due to the similarity of appearances and spatial locations between pterygiums and cortical cataracts, pterygiums are often falsely detected as cortical cataracts on retroillumination images by a computer-aided grading system. The proposed method can be used to filter out the pterygium which improves the accuracy of cortical cataract grading system. This work has three major contributions. First, we propose a new pupil segmentation method for visible wavelength images. Second, an automatic detection method of pterygiums is proposed. Third, we develop an enhanced compute-aided cortical cataract grading system that excludes pterygiums. The proposed method is tested using clinical data and the experimental results demonstrate that the proposed method can improve the existing automatic cortical cataract grading system.**

I. INTRODUCTION

A cataract is a clouding of the clear lens [1]. It has been the main cause of blindness in the world [2]. Most of cataracts are age-related and there are mainly three types, nuclear cataracts, cortical cataracts and posterior subcapsular (PSC) cataracts. Computer-aided grading systems have been proposed to facilitate clinical research and practice [3], [4], [5]. Among them, nuclear cataracts are graded using slit-lamp images and cortical and PSC cataracts are graded using retroillumination images. To capture retroillumination images, light is projected to the eye. Retina will absorb some of the projected light while the rest are reflected out through the pupil [4]. Cataracts will block the reflected light and thus they appear dark on the photograph. Besides cataracts, other opaque objects, e.g. pterygiums, in the light's path can also obstruct the reflected light to reach the camera sensor, which results in the corresponding dark region in the retroillumination images.

A pterygium is a wing-like white lesion originating from the sclera towards the cornea [1]. Fig. 1 shows the cornea image and the retroillumination image of an eye with the presence of a pterygium. It is easy to diagnose pterygiums from the cornea images. Due to the similarity of appearances and spatial locations between cortical cataracts and pterygiums on retroillumination images, pterygiums are often falsely detected as cortical cataracts for the existing computer-aided grading system. To excluding pterygiums from the detected cortical cataracts, we propose a new method to detect pterygiums using cornea images. After that, the pupil region of the cornea image and the corresponding retroillumination image are registered and the pterygium is excluded from the result of cortical cataracts.

(a) (b)

Fig. 1. An eye with a pterygium. (a) The cornea image. (b) The corresponding retroillumination image.

To detect pterygiums within the pupil region, it is necessary to segment the pupil. Pupil segmentation is also very important in iris recognition system. There are mainly three types of existing methods to segment the pupil and the iris, i.e., integrodifferential operator [6], circular Hough Transform method based on binary edge map image [7] and active contour method [8]. All the existing methods work well for the near infrared images with minimum noise. Our database consists of visible wavelength images with much noise such as cataracts in the pupil region and pterygiums in the sclera, iris and pupil regions. Furthermore, the pupil is dilated and the iris is shrunken, which blurs the boundary between the pupil and the iris. To cater for the needs of the clinical database, we propose a new pupil detection method based on color information. Ellipse fitting is utilized to make the method robust to incomplete pupil boundary caused by pterygiums. After the pupil is segmented, the pterygium within the pupil region is detected based on the color difference between the pterygium and the pupil. Finally, we align the pupil of the cornea image with the pupil of the retroillumination image and the pterygium is excluded from the detection results of cortical cataracts.

II. METHOD

A. Pupil Detection for Visible Wavelength Images

Pupils are generally black in color images for normal eyes while human irises appear in different colors. However, due to the scattering of cataract, the pupil may appear in yellow or green color as shown in Fig. 2 (a). To separate the pupils from irises well, *Fisher's linear discriminant* is applied. *Fisher's linear discriminant* projects the high dimensional

*This work was supported by A*STAR, Singapore

[1]X. Gao and W.K.D. Wong are with Department of Computer Vision and Image Understanding, Institute for Infocomm Research, A*STAR, Singapore {xgao, wkwong}@i2r.a-star.edu.sg

[2]A. W. Aryaputera and Y. Sun are with Department of Electrical and Computer Engineering, National University of Singapore, Singapore

[3]C.Y. Cheng, C. Cheung and T.Y. Wong are with Singapore Eye Research Institute, Singapore

978-1-4577-1787-1/12/$26.00 ©2012 IEEE

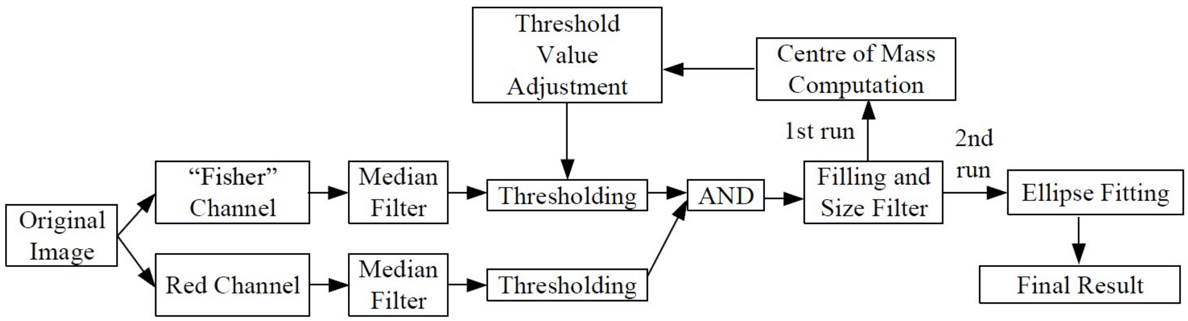

Fig. 4. The diagram of the proposed pupil detection method.

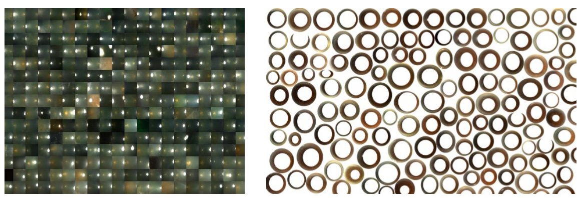

(a) (b)

Fig. 2. Training samples to learn the "Fisher" transform for pupil detection. (a) The pool image of pupils. (b) The pool image of irises.

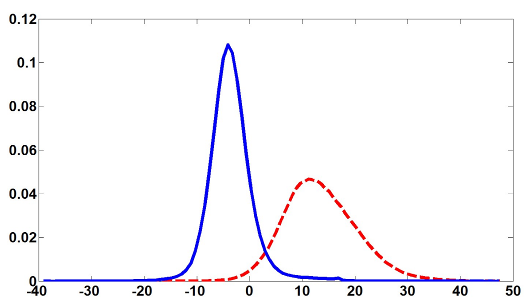

Fig. 3. Histograms of the "Fisher" images of the pool pupil image and the pool iris image shown in Fig. 2.

data onto a direction which best separates the two classes. It maximizes the ratio of the between-class variance to the within-class variance as follows.

$$J(w) = \frac{w^T S_B w}{w^T S_W w}, \tag{1}$$

where S_B represents the between-class variance and S_W represents the within-class variance. w is normal to the projection direction. $J(w)$ can be maximized by choosing w as follows.

$$w \propto S_w^{-1}(m_2 - m_1), \tag{2}$$

here, m_2 and m_1 are the mean vectors of the two classes. w is constrained to have unit length. To learn the vector w, rectangle pupil regions are cropped from 450 cornea images that are selected randomly. Coronary irises are cropped from 139 images among the 450 images used as pupil training samples. The pool images are shown in Fig. 2. Fig. 3 shows the histograms of the "Fisher" images of the pool pupil image and the pool iris image shown in Fig. 2. Using the data shown in Fig. 2, w is computed to be $[0.5952, -0.7669, 0.2402]^T$.

The cornea image is projected onto the "Fisher" direction as follows.

$$F = 0.5952 * R - 0.7669 * G + 0.2402 * B, \tag{3}$$

where R, G, B represent the intensity value in the red, green and blue channels, respectively.

The red channel and the "Fisher" channel are used to detect the pupil on the cornea images. The pupil is maximally differentiate from the iris in the "Fisher" channel. However, "Fisher" transform only maximizes the separation between the iris and the pupil, other parts of the cornea image, e.g. the sclera or the eyelids, may be mapped to have intensity values more close to the pupil than to the iris. Therefore, the red channel is needed to remove these parts. Fig. 4 shows the diagram of the proposed pupil detection method. The details of each step are as follows.

- **Step 1** Median filter is applied to the red channel image and the "Fisher" channel image to remove the noise, respectively. Then, they are thresholded.
- **Step 2** The thresholding results of the "Fisher" channel and the red channel are combined using AND operation. Then, filling and size filter operation are applied.
- **Step 3** The center of mass position of result obtained from step 2 is computed. On the "Fisher" image, the reflection is removed. A 21 by 21 square is centered at the center of mass. The adaptive threshold value for "Fisher" image is computed based on the mean value within the square.
- **Step 4** The adaptive threshold is applied to the "Fisher" image. The result is combined with the result obtained from the red channel in step 2. After filling holes and size filtering, an ellipse is fitted to the convex hull of the binary image to get the pupil segmentation.

Fig. 5 shows an example of the pupil detection method on an cornea image.

B. Pterygium Detection and the Enhanced Cortical Cataract Grading System

Pterygiums are generally white color tissue with red vessels. To detect pterygiums from cornea images, it is necessary to differentiate pterygiums from general pupils as well as pupils with the presence of cortical cataracts. We exploit color information to detect pterygiums using similar method as in pupil detection. Two transforms are learned through

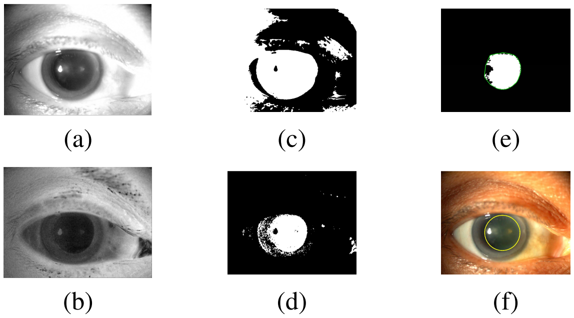

Fig. 5. An example of pupil detection for cornea images. (a) The red channel of the cornea image. (b) The "Fisher" channel of the cornea image. (c) The thresholded red channel image. (d) The thresholded "Fisher" channel image. (e) The convex hull of the detected result. (f) The final detection result.

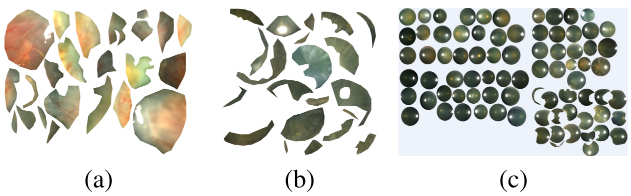

Fig. 6. Training samples to learn the "Fisher" transform for pterygium detection. (a) The pool image of pterygiums. (b) The pool image of cortical cataracts.(c) The pool image of pupils.

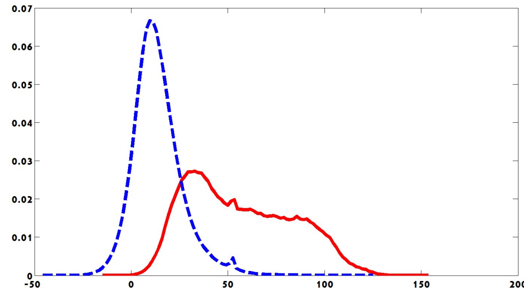

Fig. 7. Histograms of the "Fisher" images of the pool pupil image and the pool pterygium image shown in Fig. 6 (a) and (c).

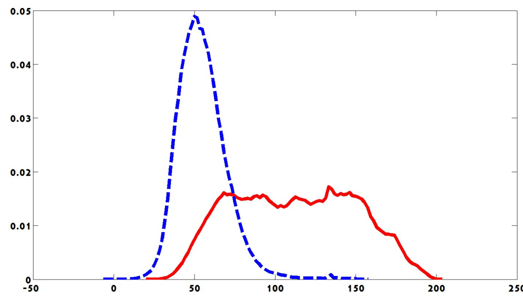

Fig. 8. Histograms of the "Fisher" images of the pool pupil image and the pool cortical cataracts image shown in Fig. 6 (a) and (b)

Fisher's linear discriminant. Training samples are extracted as follows. The pool image of pterygiums shown in Fig. 6 (a) consists of pixels of pterygiums cropped from 20 images with the presence of pterygiums. The pool image of cortical cataracts shown in Fig. 6 (b) consists of pixels of cortical cataracts cropped from 20 images with the presence of cortical cataracts. The pool image of pupils shown in Fig. 6 (c) consists of pixels of pupils extracted from 20 images of normal lens, 20 images with the presence of cortical cataracts, 20 images with the presence of PSC cataracts and the 20 images with the presence of pterygiums wherein the pterygium parts are excluded. The transform for pterygiums vs. general pupils is as follows.

$$F = 0.8863 * R - 0.4554 * G - 0.2053 * B. \quad (4)$$

Fig. 7 shows the histograms of pterygiums and general pupils in the "Fisher" image. The transform for pterygiums vs. pupils with the presence of cortical cataracts is as follows.

$$F = 0.9231 * R - 0.0136 * G - 0.3843 * B. \quad (5)$$

Fig. 8 shows the histograms of pterygiums and cortical cataracts in the "Fisher" image. Fig. 9 shows the procedure of the proposed pterygium detection method. The pupil is firstly segmented from the cornea image. Then it is resized to align with the pupil detected on the retroillumination image. The resized pupil is transformed using Eq. (4) and (5). If pterygium is detected through global thresholding, it will be compared with the detected cortical cataracts. Only the overlap part is remained as pterygium candidates. The result is further filtered by a size filter to remove noise and a spatial filter to remove the components that are not connected to the pupil boundary. If cortical cataracts are detected on an retroillumination image by the existing computer-aided system [4], the corresponding cornea image is analyzed. If pterygiums are detected on the corresponding cornea image. The detected pupil on the cornea image is resized to align with the retroillumination image. Pterygium is excluded from the corresponding part of the retroillumination image if it is detected as cortical cataracts. Fig. 10 shows an example of the proposed pterygium detection method to enhance the existing computer-aided cortical cataract grading system. The cortical cataracts are detected as 21.8206% by the existing grading system [4]. After applying the proposed pterygium excluding method, it is detected as 6.9745% which is more close the grader's grading result, 7.0266%.

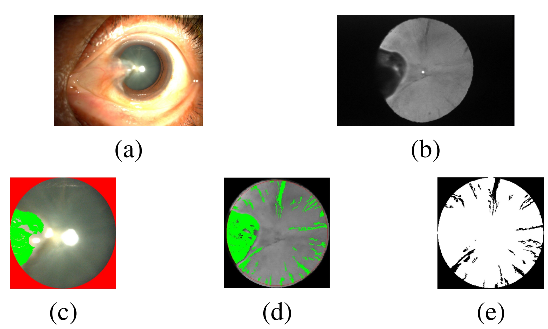

Fig. 10. An example of cortical cataracts detection with pterygium detection. (a) The cornea image. (b) The corresponding retroillumination image. (c) The pterygium detection result within the pupil region of the cornea image. (d) The cortical cataracts detection result of the existing system [4]. (e) The final cortical cataract detection result which excludes the pterygium.

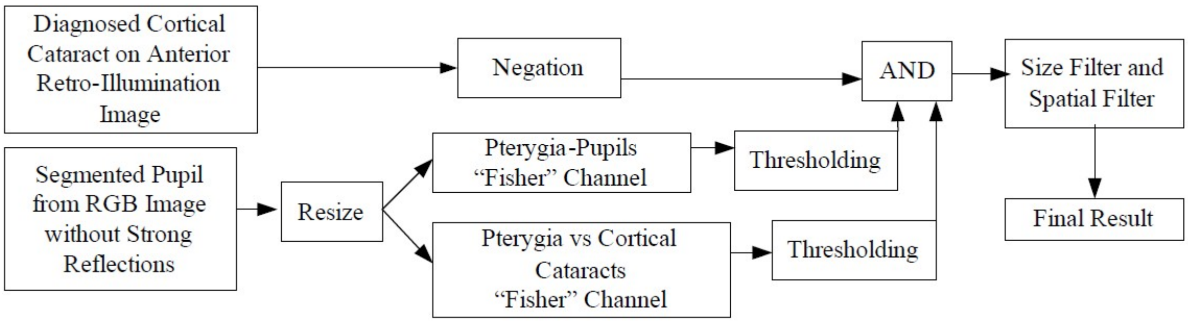

Fig. 9. The diagram of the proposed pterygium detection method.

III. Experiments

A. Database

The database is from the population based eye study, Singapore Malay Eye Study I (SiMES I). There are 7571 pairs of retroillumination and the corresponding cornea images. For pupil detection, 450 cornea images are used for learning the "Fisher" transform while the remaining 7121 images are used for testing. For pterygium detection, the proposed method is tested on 30 pterygium images and 854 non-pterygium images with the presence of cortical cataracts. Some cornea images only have early pterygium that is out of the pupil region. These images are not included in the testing of pterygium detection.

B. Pupil Detection

To compare with the widely recognized method, Daugman's integrodifferential operator, "Fisher" channel is adopted for Daugman's method too. Table I shows the results on the 7121 cornea images. Table II shows the results on the 67 cornea images with the presence of pterygiums. The results demonstrate that the proposed method is more effective and efficient for the clinical database.

TABLE I
COMPARISON BETWEEN THE PROPOSED PUPIL DETECTION METHOD AND DAUGMAN'S INTEGRODIFFERENTIAL OPERATOR

Methods	Successful Detection	Unsuccessful Detection	Success Rate(%)	Time (sec/image)
Proposed	6080	1041	85.38	3
Daugman's	4500	2621	63.19	22

TABLE II
COMPARISON BETWEEN THE PROPOSED PUPIL DETECTION METHOD AND DAUGMAN'S INTEGRODIFFERENTIAL OPERATOR ON CORNEA IMAGES WITH THE PRESENCE OF PTERYGIUMS

Methods	Successful Detection	Unsuccessful Detection	Success Rate(%)
Proposed	52	15	77.61
Daugman's	20	47	29.85

TABLE III
CONFUSION MATRIX FOR THE PROPOSED PTERYGIUM DETECTION METHOD

		Predicted Class	
		Pterygium	Non-pterygium
Actual Class	Pterygium	20	10
	Non-pterygium	168	686

C. Pterygium Detection

Table III shows the results of the proposed pterygium detection method. The positive detection rate is 66.67% and the false alarm is 19.67%.

IV. Conclusions and Discussions

In this paper, we proposed a pterygium detection method based on color information. The pupil detection method on cornea images achieves 85.38% accuracy, which is much higher than the existing method. The pterygium detector has a true positive rate of 66.67% and true negatives rate of 80.33%. An enhanced computer-aided cortical cataract diagnosis has been developed. This system excludes pterygium in the cortical cataract detection which improve the accuracy of the cortical cataracts grading system. Most of the missed cases for pterygium detection are due to the vagueness and small size of the pterygium appeared, which does not affect the cortical detection much. The pterygium detector may be improved through including the iris region in the detection.

References

[1] Kanski, J.J.: Clinical Ophthalmology - A systematic Approach. Elsevier Butterworth-Heinemann (2007)

[2] Vision2020: International agency for the prevention of blindness, 2010 report (2010)

[3] Li, H., Lim, J.H., Liu, J., Mitchell, P., Tan, A., Wang, J., Wong, T.: A computer-aided diagnosis system of nuclear cataract. IEEE Transactions on Biomedical Engineering **57**(7) (2010) 1690–1698

[4] Li, H., Ko, L., Lim, J.H., Liu, J., Wong, D.W.K., Wong, T.Y.: Image based diagnosis of cortical cataract. In: Proc. IEEE International Conference on Engineering in Medicine and Biology Society. (2008)

[5] Li, H., Lim, J.H., Liu, J., Wong, D.W.K., Foo, Y.F., Sun, Y., Wong, T.Y.: Automatic detection of PSC opacity for cataract screening. In: Proc. IEEE International Conference on Engineering in Medicine and Biology Society. (2010)

[6] Daugman, J.: High confidence visual recognition of persons by a test of statistical independence. IEEE Transactions on Pattern Analysis and Machine Intelligence **15**(11) (1993) 1148–1161

[7] Wildes, R.: Iris recognition: an emerging biometric technology. In Proceedings of the IEEE **85**(9) (1997) 1348–1363

[8] Daugman, J.: New methods in iris recognition. IEEE Transactions on Systems, Man, and Cybernetics **37**(5) (2007) 1167–1175